Letters

Modified Double-Dual-Boost High-Conversion-Ratio DC–DC Converter With Common Ground and Low-Side Gate Driving

Viet-Chan Nguyen, *Student Member, IEEE*, Honnyong Cha, *Senior Member, IEEE*, Dai-Van Bui, *Student Member, IEEE*, and Byungcho Choi, *Member, IEEE*

***Abstract*—This letter proposes a modified double-dual-boost (DDB) high-conversion-ratio dc–dc converter. The proposed converter is derived from the existing DDB converter by a simple yet effective circuit modification and inherits all the advantages of the existing DDB converter. In addition, the input and output can share a common ground due to the circuit modification, enabling the use of low-side gate drivers for all switching devices. When compared with the existing DDB converter, the proposed converter requires only one more capacitor, and the seemingly two inductors can be integrated into a single inductor. Thus, the overall magnetic volume is the same as the conventional converter. To validate the performance of the proposed converter, a 2-kW prototype was fabricated and tested.**

***Index Terms*—Common ground, double-dual-boost (DDB) converter, high-conversion ratio, interleaved, low-side gate driving.**

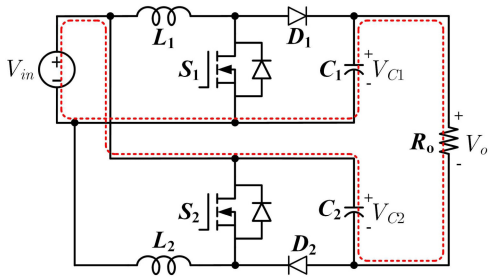

Fig. 1. Conventional DDB converter.

I. Introduction

THE INTERLEAVED boost converter (IBC) is widely used in many industrial applications due to its reduced input current ripple, reduced input/output filter size, and faster dynamics [1], [2]. However, for high-conversion-ratio applications, the IBC suffers from an extremely high duty ratio, and all switches have to withstand a high output voltage. In addition, due to the mismatches in gate signals and others, the IBC always suffers from an unbalanced inductor current. In order to balance the inductor currents, dedicated control strategies and sensing circuits are required [3]–[6].

The double-dual-boost (DDB) converter, as shown in Fig. 1, was proposed in [7]–[10]. Compared with the IBC, the DDB converter has a higher voltage gain but requires lower voltage rating switching devices [11], [12]. Because of the input-parallel output-series structure, the power sharing (or inductor current balancing) between two interleaving modules is naturally achieved without additional feedback control. However, as shown in Fig. 1, the DDB converter does not share a common ground between the input and the output, and one of the switching devices (S_2) requires a high-side gate-driving circuit. Thus, the isolated voltage sensor and the high-side gate-driving circuit should be used for feedback control and gate driving, respectively, which increase the system cost and volume and make the DDB converter less attractive to industry applications.

This letter proposes a modified DDB converter to overcome the above-mentioned shortcomings of the existing DDB converter. The proposed DDB converter is derived by simple circuit modifications and can provide a common ground and low-side gate driving for all switching devices. In addition, it inherits most of the advantages of the existing DDB converter, such as high voltage gain, low voltage stress on semiconductor devices, low input current ripple, and natural power sharing. Compared with the existing DDB converter, the proposed converter requires only one more capacitor, and the seemingly two inductors can be integrated into a single inductor. Thus, there is no increase in magnetic volume. A 2-kW hardware prototype is built and tested to verify the proposed converter's performance.

II. Topology Derivation and Operation Principle of the Proposed DDB Converter

A. Topology Derivation

Fig. 2 shows the proposed DDB converter. A step-by-step process of derivation from the existing DDB converter to the proposed converter is shown in Fig. 3 and can be described as follows.

1) [Step 1, Fig. 3(a)]: As shown in Fig. 1, the output voltage of the DDB converter is $V_o = V_{C1} + V_{C2} - V_{\rm in}$. When the inductor L_2 is moved to the positive terminal of the input, as shown in Fig. 3(a), the output voltage equation becomes $V_o = V_{C1} + V_{C2} - V_{\rm in} + v_{L2}$. The appearance of v_{L2} in the equation causes a pulsating output voltage waveform. Therefore, an *LC* filter (L_3 and C_o) is added to smoothen the output voltage.
2) [Step 2, Fig. 3(b)]: Because of the presence of C_o, the capacitors C_2 and C_o share the same ground. Thus, capacitor C_2 can be

Manuscript received September 13, 2021; revised October 29, 2021; accepted November 12, 2021. Date of publication November 26, 2021; date of current version January 19, 2022. This work was supported in part by the National Research Foundation of Korea funded by the Korea Government (MSIT) (No. NRF-2021R1A2C2007879) and in part by the Korea Evaluation Institute of Industrial Technology (Ministry of Trade, Industry, and Energy—under Grant 20012453) funded by the Korea Government. *(Corresponding author: Honnyong Cha.)*

Viet-Chan Nguyen, Honnyong Cha, and Dai-Van Bui are with the School of Energy Engineering, Kyungpook National University, Daegu 41566, South Korea (e-mail: ncviet93@gmail.com; chahonny@knu.ac.kr; buidai68@gmail.com).

Byungcho Choi is with the School of Electronics Engineering, Kyungpook National University, Daegu 41566, South Korea (e-mail: bchoi@ee.knu.ac.kr).

Color versions of one or more figures in this article are available at https://doi.org/10.1109/TPEL.2021.3130911.

Digital Object Identifier 10.1109/TPEL.2021.3130911

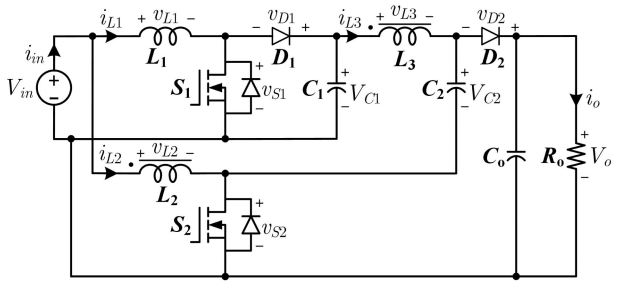

Fig. 2. Modified DDB converter.

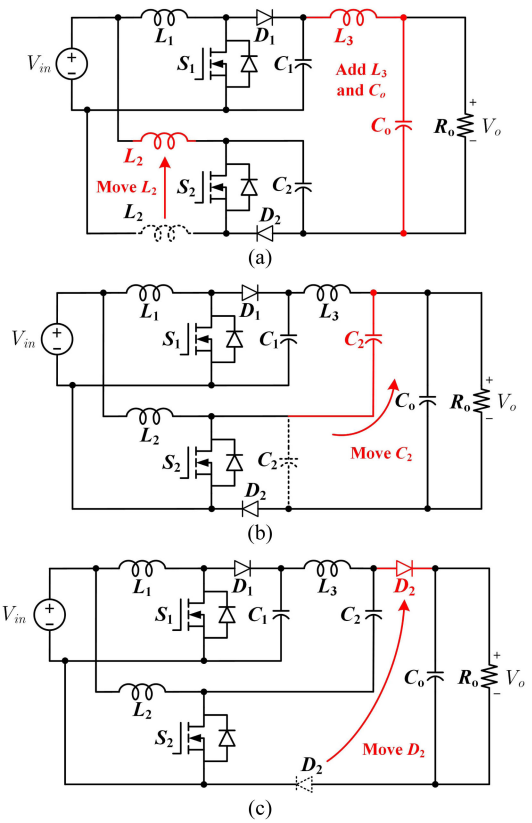

Fig. 3. Derivation of the proposed converter. (a) Step 1: Move (L_2) to the top and add L_3 and C_o. (b) Step 2: Connect C_2 to the top. (c) Step 3: Move D_2 to the top.

connected between the positive terminal of C_o and the drain terminal of S_2 without affecting the converter operation.

3) [Step 3, Fig. 3(c)]: Diode D_2 is moved to the positive terminal of C_o, as shown in Fig. 3(c), to achieve the common ground between the input and the output.

B. Operation Principle

The key waveforms of the proposed DDB converter are shown in Fig. 4, and the operation modes are depicted in Fig. 5.

1) [Mode 0, Fig. 5(a)]: All switches are turned ON, while all the diodes are turned OFF. Capacitors C_1 and C_2 are discharged and charged, respectively, through the loop C_1–L_3–C_2–S_2–V_{in}–L_1–S_1. All three inductor currents increase in this mode.
2) [Mode 1, Fig. 5(b)]: S_2 is turned OFF and D_2 is turned ON, while S_1 and D_1 are unchanged. Capacitors C_1 and C_2 discharge through the loops C_1–L_3–D_2–V_o–V_{in}–L_1–S_1 and C_2–D_2–V_o–V_{in}–L_2, respectively. In this mode, the $L1$ current increases, while the L_2 and L_3 currents decrease.
3) [Mode 2, Fig. 5(c)]: All switches are turned OFF and all diodes are turned ON. Capacitor C_1 is charged through the loop C_1–V_{in}–L_1–D_1, while C_2 discharges through the loop C_2–D_2–V_o–V_{in}–L_2. All three inductor currents decrease in this mode.
4) [Mode 3, Fig. 5(d)]: S_2 and D_1 are turned ON, while S_1 and D_2 are turned OFF. Capacitors C_1 and C_2 are charged through loops C_1–V_{in}–L_1–D_1 and C_2–S_2–V_{in}–L_1–D_1–L_3, respectively. The L_1 current decreases, while L_2 and L_3 currents increase.

TABLE I
COMPARISON OF THE EXISTING AND PROPOSED DDB CONVERTERS

DDB Converter		Existing	Proposed
Common ground		No	Yes
Low-side gate driver		One (S_1)	Two (S_1 and S_2)
Power-sharing and interleaving		Yes	
Voltage gain (V_o/V_{in})		$(1+D)/(1-D)$	
V_{C1}		$V_o/(1+D)$	
V_{C2}		$V_o/(1+D)$	$DV_o/(1+D)$
I_{L1}		$I_{in}/(1+D)$	
I_{L2}		$I_{in}/(1+D)$	$DI_{in}/(1+D)$
I_{L3}		–	$(1-D)I_{in}/(1+D)$
Voltage stress	S_1, S_2, D_1, D_2	$V_o/(1+D)$	
Current stress	S_1, S_2, D_1, D_2	$I_{in}/(1+D)$	

TABLE II
EXPERIMENTAL PARAMETERS

V_{in}/V_o	40 ~ 190 V / 400 V	C_1, C_2	40 μF
P_o	2 kW	C_o	400 μF
f_{sw}	50 kHz	S_1, S_2	IPW60R040C7
L_1	500 μH	D_1, D_2	RHRG5060
L_2, L_3/M	250, 250/240 μH	k	0.96

III. CHARACTERISTICS OF THE PROPOSED DDB CONVERTER

A. Characteristics of the Proposed Converter

From the inductor voltage waveforms (v_{L1}, v_{L2}, and v_{L3}), as shown in Fig. 4, the output and capacitor voltages of the proposed converter are obtained by applying the flux (volt-sec) balance condition on the three inductors L_1, L_2, and L_3. The results are expressed as

$$V_o = \frac{(1+D)\,V_{\text{in}}}{(1-D)} \tag{1}$$

$$V_{C1} = \frac{V_o}{(1+D)}\;;\; V_{C2} = \frac{DV_o}{(1+D)}. \tag{2}$$

From (1), (2), and the inductor voltage waveforms, as shown in Fig. 4, the instantaneous voltages of L_2 and L_3 are equal

$$v_{L2} = v_{L3}. \tag{3}$$

Similarly, from the capacitor current waveforms (i_{C1} and i_{C2}), as shown in Fig. 4, the inductor currents are calculated by applying the charge (amp-sec) balance condition on the two capacitors C_1 and C_2. The relationship of the three average inductor currents is expressed as

$$I_{L1} = I_{L2} + I_{L3}. \tag{4}$$

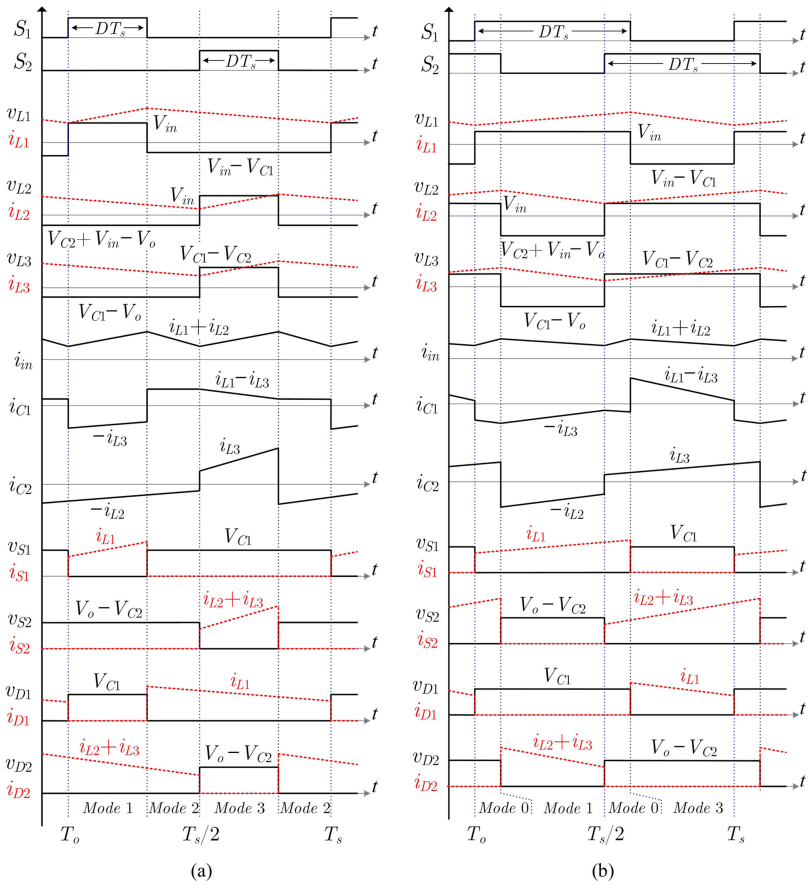

Fig. 4. Key waveforms of the proposed DDB converter. (a) When $D < 0.5$. (b) When $D > 0.5$.

From (4), the average currents for the two switches are equal ($I_{S1} = I_{S2}$), and those of the two diodes are also equal ($I_{D1} = I_{D2}$). Therefore, the intrinsic power-sharing feature is retained in the proposed converter.

B. Comparison Between the Proposed and Existing DDB Converters

Table I lists that the characteristics of the proposed and existing DDB converters are quite similar. Both converters have the same voltage gain, power-sharing function, interleaving effect in the input current, and low voltage stress on semiconductor devices. However, there are two main differences that make the proposed structure more attractive than the conventional one. First, the proposed converter shares a common ground between the converter input and output. Therefore, no isolated sensor is required for feedback control. Second, all switches of the proposed converter can be operated with the low-side gate driver. The aforementioned advantages significantly reduce the cost, size, and complexity of the proposed converter.

It should be mentioned here that although the proposed converter seems to require one more inductor (L_3) and capacitor (C_o) compared with the existing DDB converter, the two inductors L_2 and L_3 are integrated into a single inductor with exactly the same size as L_1 because the voltages across L_2 and L_3 are the same ($v_{L2} = v_{L3}$), and the sum of the currents of L_2 and L_3 ($I_{L2} + I_{L3}$) is equal to I_{L1} (see (3) and (4) in Section III-A). Thus, no increase in the magnetic volume is obtained in the proposed converter, and the proposed converter requires only one more capacitor (C_o) compared with the existing DDB converter.

C. Input Current Ripple

As shown in Fig. 2, the input current of the proposed DDB converter is the sum of i_{L1} and i_{L2}. The input current ripple can be expressed as

$$\Delta i_{\text{in}} = \frac{(1-2D)\,DV_o}{2\,(1+D)\,f}\left(\frac{L_1+L_2}{L_1L_2}\right) \text{ when } D < 0.5 \tag{5}$$

$$\Delta i_{\text{in}} = \frac{(2D-1)\,(1-D)\,V_o}{2\,(1+D)\,f}\left(\frac{L_1+L_2}{L_1L_2}\right) \text{ when } D > 0.5. \tag{6}$$

Similar to the two-phase IBC and the conventional DDB converter, the input current of the proposed DDB converter can achieve the best interleaving effect when i_{L1} and i_{L2} are 180° phase shift and $\Delta\, i_{L1} = \Delta i_{L2}$. Therefore, the inductance value of L_1 and L_2 should be equal ($L_1 = L_2 = L$) or $L_1 = L_{2\text{eq}} = L$ in case of L_2 and L_3 are coupled together.

Fig. 6 shows the ratio of input current ripple and inductor current ripple of the proposed DDB converter against duty cycle. The input current ripple comparison among the two-phase IBC, the conventional DDB converter, and the proposed DDB converter is presented in Fig. 7. Three converters are compared at the same operating condition (same input/output voltage, inductance value, and switching frequency). The input current ripple of the proposed and conventional DDB converters is the same and lower than those of two-phase IBC.

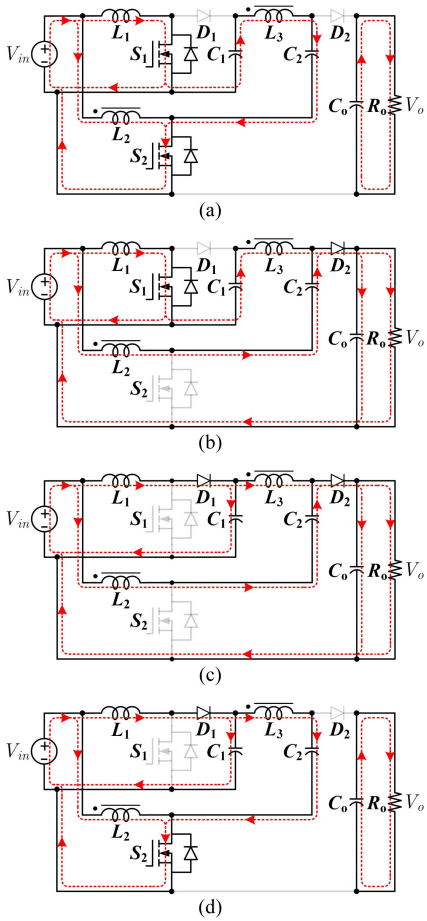

Fig. 5. Operation for (a) Mode 0, (b) Mode 1, (c) Mode 2, and (d) Mode 3.

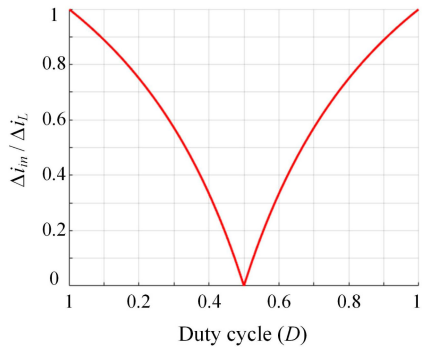

Fig. 6. Ratio of input and inductor current ripple versus duty cycle of the proposed DDB converter.

IV. Experimental Result

A 2-kW prototype of the proposed DDB converter is fabricated and tested. Fig. 8 shows the prototype photograph, and the detailed design parameters are presented in Table II. The prototype is designed to operate over a wide input voltage range (from 40 to 190 V), while the output voltage is fixed at 400 V. The inductance value of L_1 is 500 μH, while those of L_2 and L_3 are 250 μH. Because L_2 and L_3 are tightly coupled together, the effective inductances of L_2 and L_3 are 500 μH. As shown in Fig. 8, the size of the coupled inductor (L_2 and L_3) is equal to

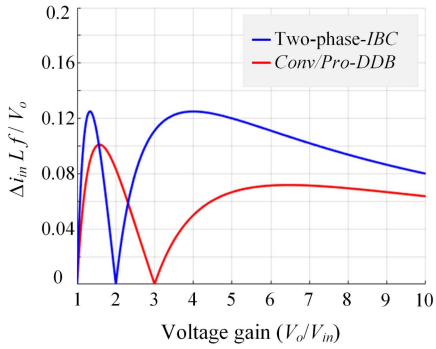

Fig. 7. Input current ripple comparison of three converters at the same voltage gain (V_o/V_{in}).

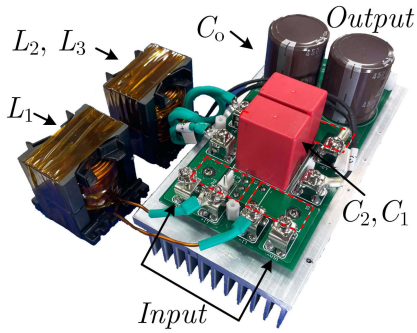

Fig. 8. Prototype photograph of the proposed DDB converter.

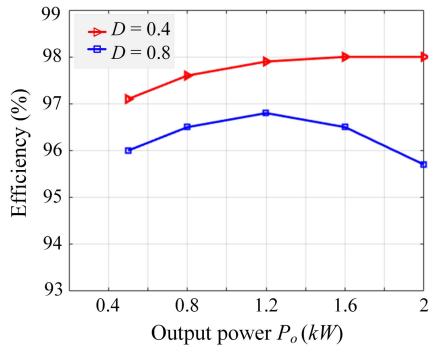

Fig. 9. Efficiency graphs of the proposed DDB converter.

that of L_1. Therefore, the magnetic volume of the proposed converter is exactly the same as that of the existing DDB converter. Fig. 9 shows the measured efficiency. The peak efficiency of the converter is 98% at D = 0.4. Fig. 10(a) shows the experimental waveforms of the switching device voltages and inductor currents at $D = 0.4$, $V_{\text{in}} = 170$ V, $V_o = 400$ V, and $P_o = 2$ kW. Fig. 10(b) shows the same waveforms at $D = 0.8$, $V_{\text{in}} = 45$ V, $V_o = 400$ V, and $P_o = 2$ kW. As shown, the voltage stresses of all semiconductor devices are lower than the output voltage. Due to the interleaving effect, the input current ripple is reduced, and its frequency is twice as high as the switching frequency.

V. Conclusion

This letter proposed a modified DDB converter. The following points are the features of the proposed converter.

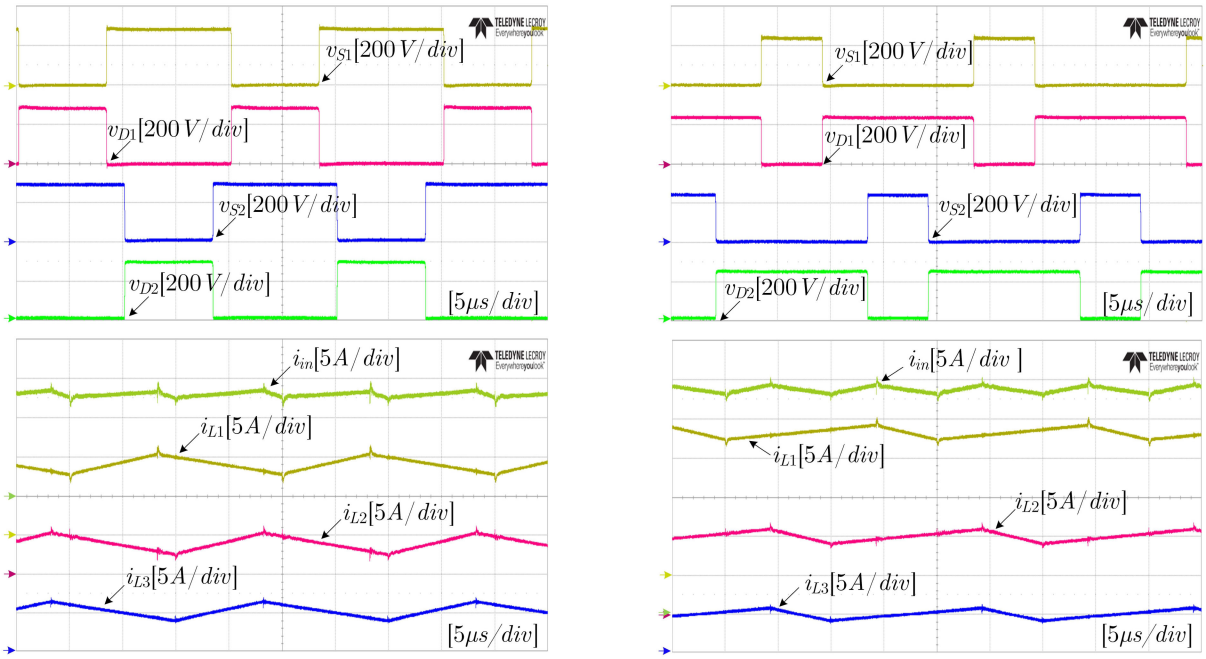

Fig. 10. Experimental waveforms of the proposed DDB converter. (a) $D = 0.4$ ($V_{\rm in} = 170$ V, $V_o = 400$ V, and $P_o = 2$ kW). (b) $D = 0.8$ ($V_{\rm in} = 45$ V, $V_o = 400$ V, and $P_o = 2$ kW).

1) The proposed converter has the same high voltage gain and low voltage stresses on semiconductor devices as the existing DDB converter.
2) It retains the same interleaving and power-sharing function as the existing DDB converter.

Moreover, the proposed converter has the following additional features that cannot be obtained in the existing DDB converter.

1) The input and output of the converter share a common ground.
2) All switches of the proposed converter can be operated with the low-side gate driver.

A detailed analysis of the proposed DDB converter was provided. Accordingly, the converter's performance was verified using a 2-kW prototype.

REFERENCES

[1] T.-R. Granados-Luna *et al.*, "Two-phase, dual interleaved buck–boost dc–dc converter for automotive applications," *IEEE Trans. Ind. Appl.*, vol. 56, no. 1, pp. 390–402, Jan./Feb. 2020.

[2] S. Abedinpour, B. Bakkaloglu, and S. Kiaei, "A multistage interleaved synchronous buck converter with integrated output filter in 0.18 μm SiGe process," *IEEE Trans. Power Electron.*, vol. 22, no. 6, pp. 2164–2175, Nov. 2007.

[3] S. Chae, Y. Song, S. Park, and H. Jeong, "Digital current sharing method for parallel interleaved dc–dc converters using input ripple voltage," *IEEE Trans. Ind. Informat.*, vol. 8, no. 3, pp. 536–544, Aug. 2012.

[4] T. Ohata and T. Saito, "Stability analysis of multi-phase synchronization in paralleled buck converters with winner-take-all and loser-take-all switching rules," *IEEE J. Emerg. Sel. Topics Circuits Syst.*, vol. 5, no. 3, pp. 345–353, Sep. 2015.

[5] M. Sun, Z. Yang, K. Joshi, D. Mandal, P. Adell, and B. Bakkaloglu, "A 6 A, 93% peak efficiency, 4-phase digitally synchronized hysteretic buck converter with $\pm$1.5% frequency and $\pm$3.6% current-sharing error," *IEEE J. Solid-State Circuits*, vol. 52, no. 11, pp. 3081–3094, Nov. 2017.

[6] C.-J. Chen, Z.-Y. Zeng, C.-H. Cheng, and F.-T. Lin, "Comprehensive analysis and design of current-balance loop in constant on-time controlled multi-phase buck converter," *IEEE Access*, vol. 8, pp. 184752–184764, 2020.

[7] D. B. Viet, Y. Lembeye, J. P. Ferrieux, J. Barbaroux, and Y. Avenas, "New high power—High ratio non isolated dc–dc boost converter for fuel cell applications," in *Proc. 37th IEEE Power Electron. Specialists Conf.*, 2006, pp. 1–7.

[8] F. Forest *et al.*, "A nonreversible 10-kW high step-up converter using a multicell boost topology," *IEEE Trans. Power Electron.*, vol. 33, no. 1, pp. 151–160, Jan. 2018.

[9] F. S. Garcia, J. A. Pomilio, and G. Spiazzi, "Modeling and control design of the interleaved double dual boost converter," *IEEE Trans. Ind. Electron.*, vol. 60, no. 8, pp. 3283–3290, Aug. 2013.

[10] C. A. Villarreal-Hernandez, J. C. Mayo-Maldonado, G. Escobar, J. Loranca-Coutino, J. E. Valdez-Resendiz, and J. C. Rosas-Caro, "Discrete-time modeling and control of double dual boost converters with implicit current ripple cancellation over a wide operating range," *IEEE Trans. Ind. Electron.*, vol. 68, no. 7, pp. 5966–5977, Jul. 2021.

[11] M. Kabalo, D. Paire, B. Blunier, D. Bouquain, M. G. Simoes, and A. Miraoui, "Experimental validation of high-voltage-ratio low-input-current-ripple converters for hybrid fuel cell supercapacitor systems," *IEEE Trans. Veh. Technol.*, vol. 61, no. 8, pp. 3430–3440, Oct. 2012.

[12] M. Esteki, B. Poorali, E. Adib, and H. Farzanehfard, "Interleaved buck converter with continuous input current, extremely low output current ripple, low switching losses, and improved step-down conversion ratio," *IEEE Trans. Ind. Electron.*, vol. 62, no. 8, pp. 4769–4776, Aug. 2015.